Performance Analysis and Optimization of OFDM Receiver With Blanking Nonlinearity in Impulsive Noise Environment

Sergey V. Zhidkov

***Abstract*—A simple method of improving orthogonal frequency division multiplexing (OFDM) receiver performance in an impulsive noise environment is to precede a conventional OFDM demodulator with blanking nonlinearity. This method is widely used in practice since it is efficient and very simple to implement. However, performance analysis of this scheme has not yet appeared. In this paper, we study performance of the OFDM receiver with blanking nonlinearity in the presence of impulsive noise. Closed form analytical expressions for the signal-to-noise ratio (SNR) at the output of blanking nonlinearity and the optimal blanking threshold that maximizes SNR are derived. Simulation results are provided that show good agreement with theory if the number of OFDM subcarriers is sufficiently large.**

***Index Terms*—Blanking nonlinearity, impulsive noise, multicarrier modulation, orthogonal frequency division multiplexing (OFDM).**

I. Introduction

ORTHOGONAL frequency division multiplexing (OFDM) is an effective multicarrier transmission scheme suitable for high data rate wireless applications. OFDM has several advantages over single-carrier systems, particularly its robustness to multipath propagation, and efficient implementation based on fast Fourier transform (FFT) [1]. One of the challenging problems in practical applications of wireless digital communication techniques is data transmission over channels with man-made noise that appears in typical urban environments. The man-made noise created by vehicle ignition systems, power lines, heavy current switches, and other sources cannot be assumed to be Gaussian, and must be represented by impulsive models [2]–[6].

In general, OFDM systems are less sensitive to impulsive noise than single carrier systems. The longer OFDM symbol duration provides an advantage, since the impulsive noise energy is spread among simultaneously transmitted OFDM subcarriers. However, it has been recently recognized that this advantage turns into a disadvantage if impulsive noise energy exceeds a certain threshold [7], [8]. A simple method of reducing the adverse effect of impulsive noise is to precede a conventional OFDM demodulators with blanking nonlinearity. This method is widely used in practice, because it is very simple to implement and provides an improvement over conventional OFDM demodulators in impulsive noise channels [8]–[10]. However, performance analysis of this scheme has not yet appeared. In this paper, we address the problem of optimal threshold selection and performance characterization of an OFDM receiver that uses blanking nonlinearity for impulsive noise cancellation.

It should be noted that the idea of using blanking nonlinearity (also referred to as a blanker or hole puncturer) for impulsive noise cancellation is not new. It was shown over four decades ago that the locally optimal detector for arbitrary signals in impulsive noise under a low signal-to-noise ratio (SNR) assumption is comprised of a conventional detector (optimal in a Gaussian noise environment) preceded by a memoryless nonlinearity [11], [12]. Generally, the shape of the optimal memoryless nonlinearity is determined by the probability density function of the impulsive noise process [11], [12]. However, it is shown that the blanking nonlinearity is one of the best (and the simplest) approximations to the locally optimal nonlinear preprocessor [13], [14]. Recently, the idea of using (suboptimal) blanking nonlinearity for impulsive noise cancellation has been successfully applied to modern OFDM communication systems [8]–[10].

It should also be noted that the performance of receivers with blanking nonlinearity was analyzed in [13]–[16]. However, the analysis presented in [13]–[15] relies on a weak signal assumption, which is not valid for most of the modern OFDM systems in a typical impulsive noise environment. Moreover, the performance studies carried out in the past were based on computer simulations [13], [16], or numerical methods [14].

Unlike the previous studies, in this paper, we provide theoretical analysis that does not rely on the small signal assumption. The only assumption made is that the OFDM signal with large number of subcarriers can be modeled as a complex Gaussian process with Rayleigh envelope distribution [17]–[19].

The primary objectives of this study are

1) to find the optimal blanking threshold for the OFDM receiver with blanking nonlinearity under various impulsive noise scenarios;
2) to determine the worst-case impulsive noise scenario for the OFDM receiver with blanking nonlinearity.

These two problems are essential for the development of practical adaptive receivers (i.e., receivers that use adaptive blanking threshold) and for laboratory tests of the OFDM receivers employing blanker or other techniques for impulsive noise cancellation. The performance of the optimized OFDM receiver with blanker can also serve as a benchmark for comparison with more sophisticated impulsive noise cancellation techniques (e.g., [19] and [20]).

Manuscript received May 25, 2004; revised November 5, 2004, January 15, 2005, and February 13, 2005. The review of this paper was coordinated by Dr. Z. Xu.

The author is with the System-on-Chip Research Center, Samsung Electronics Co. Ltd., Giheung, Korea 449-711 (e-mail: s.zhidkov@samsung.com).

Digital Object Identifier 10.1109/TVT.2005.858191

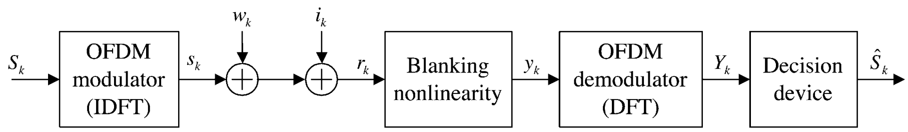

Fig. 1. Block-scheme of transmission system.

Two additional remarks are given as follows. First, the analysis presented in this paper is based on the assumption that the input OFDM signal can be modeled as a complex Gaussian process. Therefore, the analysis remains valid for other kinds of communication signals that can be modeled as a complex Gaussian process, for example, code-division multiplexing signals [21]. Second, the paper mainly focuses on the specific impulsive noise model (two-component mixture-Gaussian distribution). However, as shown in Section VI, the analysis can also be extended to a general case of mixture-Gaussian noise distribution, which is a very flexible tool for modeling various non-Gaussian noise sources [22].

The paper is organized as follows. In Section II, the system model is introduced. In Section III, the signal-to-noise ratio at the output of blanking nonlinearity is derived, and numerical results are provided. The threshold optimization strategy is considered in Section IV. In Section V, we discuss the problem of symbol error rate estimation in OFDM receiver with blanking nonlinearity. Some numerical examples and simulation results are also provided in Section V. In Section VI, it is shown that the results can be extended to the multicomponent mixture Gaussian noise model. Finally, Section VII presents conclusions.

II. System Model

Consider the model of the OFDM transmission system shown in Fig. 1. First, in the OFDM transmitter, information bits are mapped into baseband symbols S_k using phase shift keying (PSK), or a quadrature amplitude modulation (QAM) scheme. During an active symbol interval, the block of N complex baseband symbols is transformed by means of inverse discrete Fourier transform (DFT) and digital-to-analog conversion to the complex baseband OFDM signal as [23, p. 719]

$$s(t) = \frac{1}{\sqrt{N}} \sum_{k=0}^{N-1} S_k e^{j\frac{2\pi k t}{T_s}}, \quad 0 < t < T_S \tag{1}$$

where N is the number of subcarriers, and T_S is the active symbol interval. The time domain received signal after down-conversion, analog-to-digital conversion, and perfect synchronization can be expressed as

$$r_k = s_k + w_k + i_k, \quad k = 0, 1, \ldots, N-1 \tag{2}$$

where $s_k = s(kT_S/N)$, w_k is the additive white Gaussian noise (AWGN), and i_k is the impulsive noise (s_k, w_k and i_k are assumed to be mutually independent).

In this study, we assume that the impulsive noise can be modeled as a Bernoulli–Gaussian random process [7]

$$i_k = b_k g_k, \quad k = 0, 1, \ldots, N-1 \tag{3}$$

where b_k is the Bernoulli process, i.e., an independent and identically distributed sequence of zeros and ones with probability $P(b_k = 1) = p$, and g_k is the complex zero-mean white Gaussian noise. We assume that the additive white Gaussian noise (AWGN) has variance $\sigma_w^2 = (1/2)E[|w_k|^2]$, and the variance of the Gaussian component of the impulsive noise is $\sigma_g^2 = (1/2)E[|g_k|^2]$. Without loss of generality, we also assume that the OFDM signal power is normalized as $\sigma_s^2 = (1/2)E[|s_k|^2] = 1$.

The noise term $u_k = w_k + i_k$ in (2) can also be expressed in terms of the two-component mixture-Gaussian model, which is widely accepted and frequently used for performance analysis of various transmission schemes in an impulsive noise environment [7], [24]–[26]. As mentioned in the introduction, the analysis can also be extended to the general case of multicomponent mixture-Gaussian distribution. In such a case, the analysis is essentially the same as the analysis of twocomponent mixture-Gaussian model; therefore, this model is briefly considered in Section VI.

To reduce energy of the impulsive noise, the blanking nonlinearity can be applied to the received baseband signal r_k before the conventional OFDM demodulator (see, for example [9], [10], and [16])

$$y_k = \begin{cases} r_k, & \text{if } |r_k| < T \\ 0, & \text{otherwise} \end{cases}, \quad k = 0, 1, \ldots, N-1 \tag{4}$$

where T is the threshold value.

Nonlinearity (4) reduces the effect of large received signal values, as these are assumed to be the result of impulsive noise. Finally, signal samples y_k are fed to a conventional DFT-based OFDM demodulator, as shown in Fig. 1.

III. Signal-to-Noise Ratio at the Output of Blanking Nonlinearity

A. SNR Definition

To assess receiver performance, we should first represent the output of a nonlinear preprocessor (4) as

$$y_k = K_0 s_k + d_k, \quad k = 0, 1, \ldots, N-1 \tag{5}$$

where the first term on the right-hand side of (5) represents the scaled replica of information-bearing signal, d_k as the cumulative noise/distortion term, and K_0 is the appropriately chosen scaling factor. It is usually desirable to have a zero-mean noise process $(d_k = y_k - K_0 s_k)$ uncorrelated with the useful signal; i.e., $E[d_k s_k^*] = 0$. In case of the transmitter nonlinearity analysis, this decomposition is justified by Bussgang's theorem and permits the utilization of a simple additive model to analyze the joint effect of transmitter nonlinearity and channel noise [18], [21].

The optimal scaling factor in (5), which satisfies $E[d_k s_k^*] = 0$, can be found as [18]

$$K_0 = \frac{E[y_k s_k^*]}{E[|s_k|^2]} = \frac{1}{2} E[y_k s_k^*]. \quad (6)$$

When K_0 is chosen in accordance with (6), the signal-to-noise ratio (SNR) after impulsive noise preprocessing can be expressed as

$$\gamma = \frac{E[|K_0 s_k|^2]}{E[|y_k - K_0 s_k|^2]} = \left(\frac{E[|y_k|^2]}{2K_0^2} - 1 \right)^{-1} \quad (7)$$

where $E[|y_k|^2]$ represents the total signal power (i.e., the useful signal power plus noise/distortion power) at the output of blanking nonlinearity. The derivation of K_0 and $E[|y_k|^2]$ will be considered in Section III-B.

In accordance with the system model presented in Section II, s_k, w_k and i_k are mutually uncorrelated white spectrum sequences. Therefore, the noise process d_k is also white, and SNR is constant for all OFDM subchannels. Note that SNR (7) can also be used to characterize the output of the OFDM demodulator, since the SNR at the input of the OFDM demodulator (DFT) and SNR at its output are equal (see, for example, [19]).

The following analysis relies on the assumption that the number of OFDM subcarriers is sufficiently large ($N \to \infty$), and the OFDM signal can be modeled as a complex Gaussian process with Rayleigh envelope distribution [17]–[19]. To enable symbol error rate (SER) estimation, some additional assumptions will be introduced in Section V.

B. Optimal Scaling Factor and the Total Signal Power at the Output of Blanking Nonlinearity

Using representation of the signal at the output of blanking nonlinearity given by (4), it is straightforward to express (6) as

$$\begin{aligned} K_0 &= \frac{1}{2} E[(s_k + w_k) s_k^* | \bar{C}, \bar{I}] P(\bar{C}, \bar{I}) \\ &\quad + \frac{1}{2} E[(s_k + w_k + g_k) s_k^* | \bar{C}, I] P(\bar{C}, I) \\ &= \frac{1}{2} E[|s_k|^2 | \bar{C}, \bar{I}] P(\bar{C}, \bar{I}) + \frac{1}{2} E[|s_k|^2 | \bar{C}, I] P(\bar{C}, I) \\ &\quad + \frac{1}{2} E[w_k s_k^* | \bar{C}, \bar{I}] P(\bar{C}, \bar{I}) \\ &\quad + \frac{1}{2} E[(w_k + g_k) s_k^* | \bar{C}, I] P(\bar{C}, I) \end{aligned} \quad (8)$$

where C is the event of clipping a signal above level T, and I is the event of impulse noise occurring ($\bar{C}$ and $\bar{I}$ are their complements).

Joint probabilities $P(\bar{C}, \bar{I})$, $P(\bar{C}, I)$ can easily be expressed analytically due to the fact that the amplitude of received samples (r_k) is Rayleigh-distributed. In particular, if received sample r_k is not contaminated with impulsive noise, A_r has a Rayleigh distribution with parameter $\sigma^2 = 1 + \sigma_w^2$, and hence, joint probability $P(\bar{C}, \bar{I})$ can be expressed as

$$\begin{aligned} P(\bar{C}, \bar{I}) &= P(A_r < T | \bar{I})(1 - p) \\ &= (1 - p) \left(1 - e^{-\frac{T^2}{2(1+\sigma_w^2)}} \right). \end{aligned} \quad (9)$$

On the other hand, if a received sample is affected by impulsive noise, A_r has a Rayleigh distribution with parameter $\sigma^2 = 1 + \sigma_w^2 + \sigma_g^2$, and, as a consequence, $P(\bar{C}, I)$ is expressed as

$$P(\bar{C}, I) = P(A_r < T | I) p = p \left(1 - e^{-\frac{T^2}{2\left(1+\sigma_w^2+\sigma_g^2\right)}} \right). \quad (10)$$

The derivation of the conditional expectations $E[|s_k|^2 \,|\, \bar{C}, \bar{I}/I]$, $E[w_k s_k^* \,|\, \bar{C}, \bar{I}]$ and $E[(w_k + g_k) s_k^* | \bar{C}, I]$ is given in Appendix I. Combining these results yields the following closed-form expression for K_0 :

$$\begin{aligned} K_0 = 1 &- \left(1 + \frac{T^2}{2\left(1 + \sigma_w^2\right)} \right) (1 - p) e^{-\frac{T^2}{2(1+\sigma_w^2)}} \\ &- \left(1 + \frac{T^2}{2\left(1 + \sigma_w^2 + \sigma_g^2\right)} \right) p e^{-\frac{T^2}{2\left(1+\sigma_w^2+\sigma_g^2\right)}}. \end{aligned} \quad (11)$$

It is worth noting that the optimal K_0 is a real constant, which means that the signal constellation at the input of the decision device is not rotated. On the other hand, there is constellation shrinking after blanking nonlinearity, since $K_0 \leq 1$.

The total signal power at the output of blanking nonlinearity can be expressed as

$$E[|y_k|^2] = E[|y_k|^2 \,|\, \bar{C}, \bar{I}] P(\bar{C}, \bar{I}) + E[|y_k|^2 \,|\, \bar{C}, I] P(\bar{C}, I). \quad (12)$$

The analytical derivation of the conditional expectations $E[|y_k|^2 \,|\, \bar{C}, \bar{I}/I]$ is summarized in Appendix II. Combining the results given in Appendix II with (9)–(10), and (12) yields the following closed-form expression for $E[|y_k|^2]$:

$$\begin{aligned} E[|y_k|^2] &= 2\left(1 + \sigma_w^2 + p\sigma_g^2\right) \\ &\quad - (1 - p)\left\{T^2 + 2\left(1 + \sigma_w^2\right)\right\} e^{-\frac{T^2}{2(1+\sigma_w^2)}} \\ &\quad - p\left\{T^2 + 2\left(1 + \sigma_w^2 + \sigma_g^2\right)\right\} e^{-\frac{T^2}{2\left(1+\sigma_w^2+\sigma_g^2\right)}}. \end{aligned} \quad (13)$$

Finally, substituting (11) and (13) in (7) results in a closed form expression for SNR at the output of blanking nonlinearity (4). It is interesting to note that in the limiting case $T \to \infty$, SNR (7) approaches

$$\lim_{T \to \infty} \gamma = \frac{1}{\sigma_w^2 + p\sigma_g^2} \quad (14)$$

as would be in case with a conventional OFDM receiver.

Output SNR as a function of the threshold value is illustrated in Fig. 2 along with some simulation results for OFDM systems with a finite number of subcarriers. In all figures, SNR is defined as

$$\mathrm{SNR} = 10 \log_{10} \left(\frac{1}{\sigma_w^2} \right) \quad (15)$$

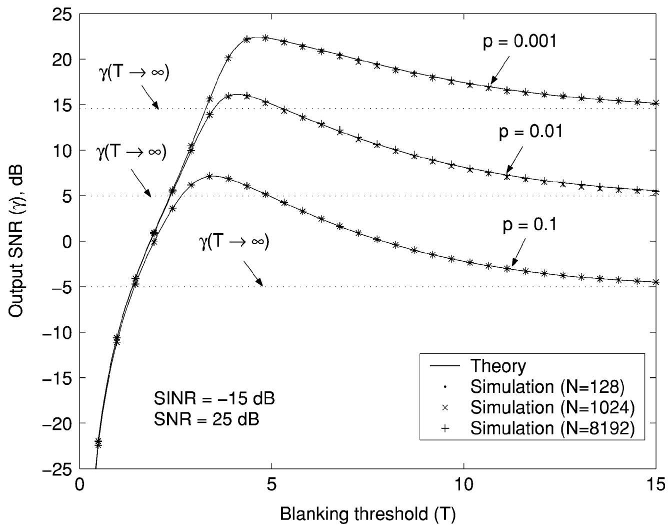

Fig. 2. SNR at the output of blanking nonlinearity versus threshold value (simulation results for 16-QAM system).

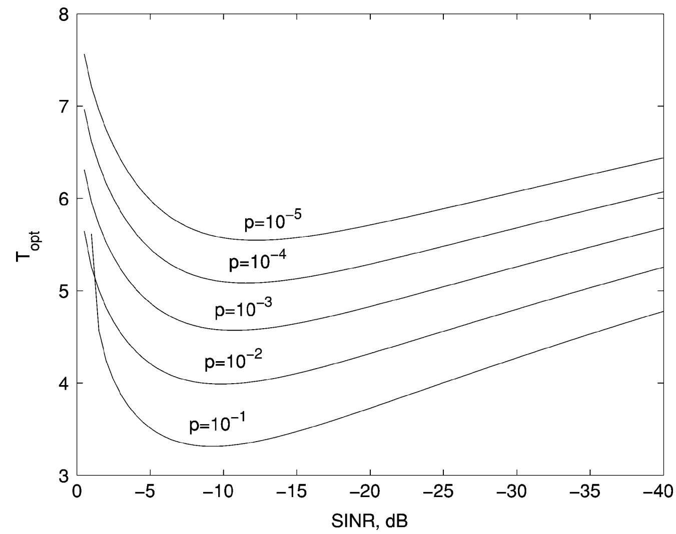

Fig. 3. Optimal threshold value versus signal-to-impulsive noise ratio $(\mathrm{SNR} = 40$ dB).

and signal-to-impulsive noise ratio (SINR) is defined as

$$\mathrm{SINR} = 10\log_{10}\left(\frac{1}{\sigma_g^2}\right). \tag{16}$$

As one can see, simulation results are in perfect agreement with theory even when the number of subcarriers is relatively small.

IV. Threshold Optimization

Output SNR (7) is a nonmonotonic function of the threshold value (T). When T is too small, a significant portion of the OFDM signal is replaced with zeros and, as a result, the output SNR is significantly decreased. On the other hand, if T approaches infinity, the impulsive noise may considerably degrade system performance. As a consequence, there is an optimal threshold value T_{opt} that maximizes output SNR (7) (see, for example, Fig. 2). The optimal threshold value (T_{opt}) can be found as the solution of the equation

$$\frac{\partial}{\partial T}\left\{\frac{E[|y_k|^2]}{K_0^2}\right\} = 0. \tag{17}$$

Computationally, it is more desirable to take the logarithm of $E[|y_k|^2]/K_0^2$ and replace (17) with an equivalent equation

$$\frac{\partial \ln E[|y_k|^2]}{\partial T} - 2\frac{\partial \ln K_0}{\partial T} = 0. \tag{18}$$

Derivatives on the left-hand side of (18) can easily be evaluated analytically [see (25), for example]. Nevertheless, the solution of (18) cannot be expressed in a simple closed form. Fortunately, the numerical solution of (18) does not pose any computational difficulties. For instance, some numerical results are presented in Fig. 3, where the optimal threshold value is plotted versus the signal-to-impulsive noise ratio (SINR). Also, in Fig. 4, the output SNR corresponding to the optimal threshold T_{opt} is plotted versus SINR. It is interesting to note that for given probability p, there is a worst case SINR that minimizes output SNR (7). This phenomenon can be explained as follows. If SINR approaches zero and an appropriate (optimal) value of T is used in (4), all of the impulsive noise samples can be detected and replaced with zeros, whereas signal samples unaffected by impulsive noise remain unclipped (ideal impulse detection). It is easy to show that in this case, $K_0 \to (1-p)$, $E[|y_k|^2] \to 2(1-p)[1+\sigma_w^2]$, and the SNR at the output of blanker can be approximated as

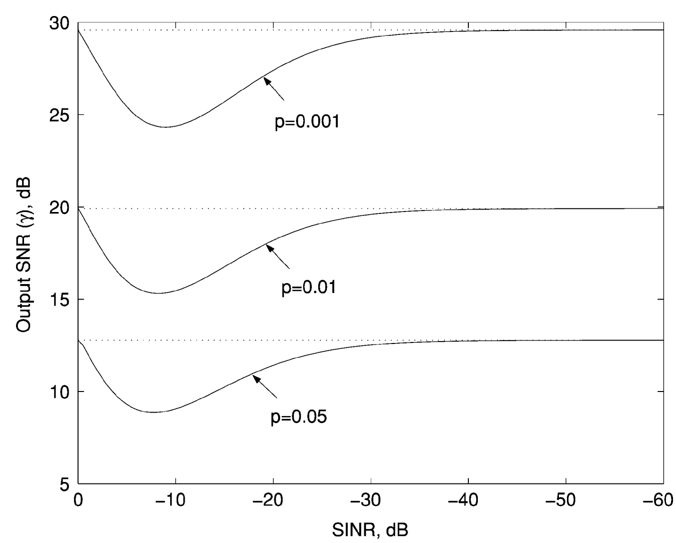

Fig. 4. Maximum achievable SNR at the output of blanking nonlinearity versus signal-to-impulsive noise ratio $(\mathrm{SNR} = 40$ dB, dashed line: approximation (32)).

$$\lim_{\substack{\sigma_g^2 \to \infty \\ T = T_{\mathrm{opt}}}} \gamma = \left(\frac{1-\sigma_w^2}{1-p} - 1\right)^{-1}. \tag{19}$$

On the other hand, approximation (19) is only valid for extremely low SINR values, which are rarely encountered in practice. If SINR value is intermediate the actual receiver performance may be worse than that predicted by (19). It is seen from Fig. 4 that the receiver with blanking nonlinearity exhibits the worst

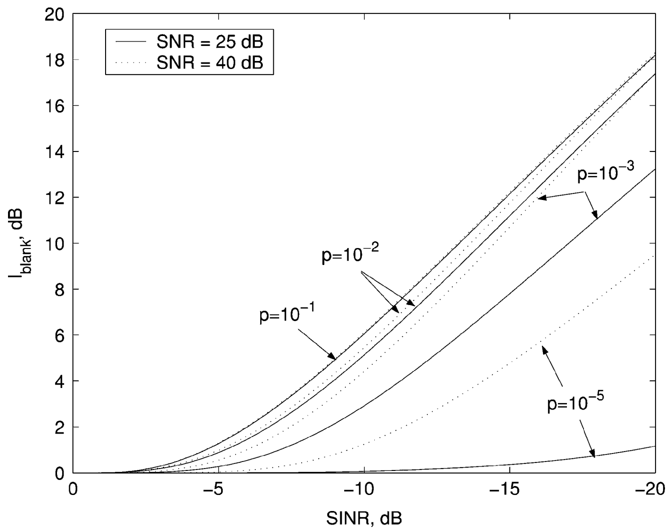

Fig. 5. Improvement in OFDM receiver with blanking nonlinearity versus signal-to-impulsive noise ratio.

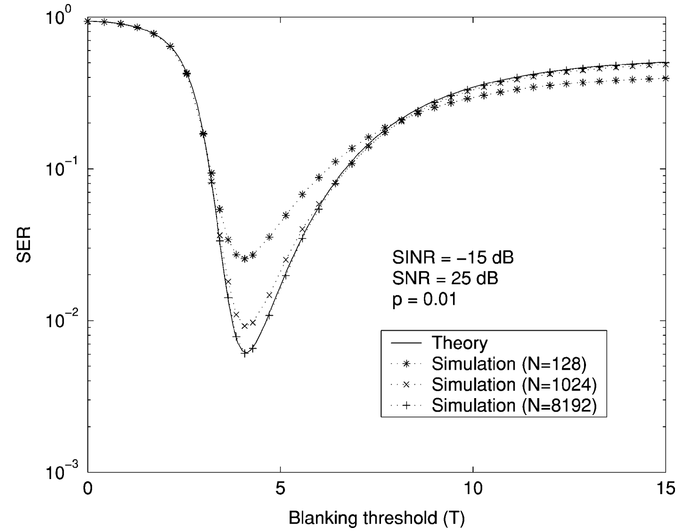

Fig. 6. Symbol error rate at the output of 16-QAM-OFDM demodulator versus threshold value (theoretical results using Gaussian approximation and simulation results for finite number of subcarriers).

performance in the intermediate SINR region (-6 dB $\ldots -9$ dB). The difference in terms of the output SNR can be up to 6 dB for given examples (Fig. 4) compared with the case of SINR $\rightarrow 0$.

An improvement over the conventional (linear) receiver that can be achieved in the OFDM receiver with blanking nonlinearity is expressed as

$$I_{\text{blank}} = 10 \log_{10} \left(\frac{\gamma(T \rightarrow \infty)}{\gamma(T = T_{\text{opt}})} \right). \tag{20}$$

Improvement (20) as a function of SINR is illustrated in Fig. 5 for two SNR values and several probabilities of impulse occurrence p. It can be observed that the improvement is larger if the probability of impulse occurrence is high and SINR is low. Note that the valuable performance improvement can only be achieved if SINR ≤ -3 dB; for greater SINR values, blanking nonlinearity provides negligible performance improvement.

V. SER Estimation

The exact evaluation of the symbol or bit error probability in the OFDM receiver with blanking nonlinearity is quite a difficult task. Fortunately, due to the central limit theorem the noise at the output of an OFDM demodulator (DFT) approaches Gaussian distribution when the number of subcarriers is sufficiently large. This fact is well-known and widely used in the analysis of multicarrier systems [8], [9], and [21]. Thus property of an OFDM demodulator (DFT) permits using a Gaussian approximation of the noise distribution in order to estimate the symbol error probability in the OFDM system with blanking nonlinearity. However, there is one important property of the OFDM receiver with blanking nonlinearity that should be taken into account: if only few samples within an OFDM symbol interval are affected by impulsive noise, the noise at the output of OFDM demodulator may not approach Gaussian distribution even when the number of subcarriers is sufficiently large. Therefore, noise at

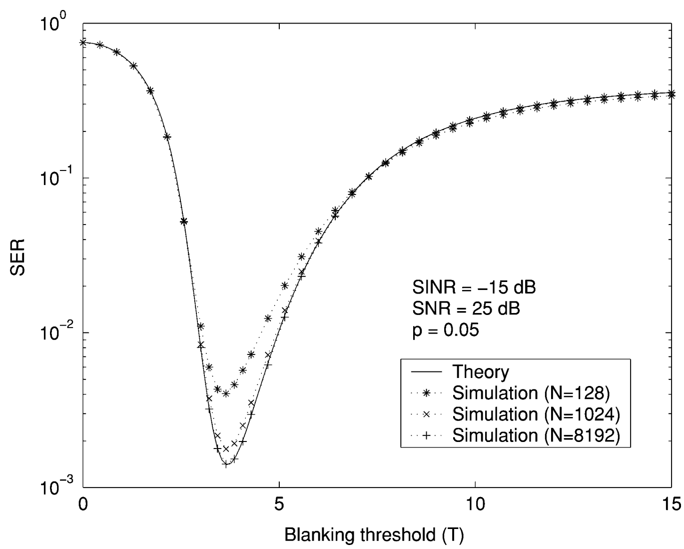

Fig. 7. Symbol error rate at the output of QPSK-OFDM demodulator versus threshold value (theoretical results using Gaussian approximation and simulation results for finite number of subcarriers).

the input of the decision device can be viewed as an uncorrelated white Gaussian process only if $Np \gg 1$. These considerations are illustrated by simulation results shown in Figs. 6 and 7. The theoretical curves are obtained using the well-known result for the m-QAM symbol error probability in the AWGN channel, [23, p. 278]

$$P_S = 1 - \left[1 - 2 \left(1 - \frac{1}{\sqrt{m}} \right) Q \left(\sqrt{\frac{3\gamma}{m-1}} \right) \right]^2 \tag{21}$$

where m is the constellation order $m = 2^{2k}, k = 1, 2, \ldots, \gamma$ is the SNR (7), and $Q(x)$ is the Gaussian Q-function [23]. As one can see, the theoretical SER prediction is in perfect agreement with theory when $Np > 10$. On the other hand, for $Np \approx 1$, prediction is rather loose, especially for high threshold values ($T > 3$).

VI. Extension to the Multicomponent Mixture-Gaussian Noise Model

The previous analysis can easily be extended to the general case of the multicomponent mixture-Gaussian noise model [22]. Let us consider the model of transmission system (2) where the probability density function of the noise samples ($u_k = w_k + i_k$) is given by

$$f(u_k) = \sum_{l=0}^{L-1} p_l g(u_k \mid \sigma_l^2) \tag{22}$$

where $g(u_k \mid \sigma^2)$ is the probability density function of the complex Gaussian process with zero-mean and variance σ^2, $\{p_0, p_1, \ldots, p_{L-1}\}$, and $\{\sigma_0, \sigma_1, \ldots, \sigma_{L-1}\}$ are the model parameters, and the condition $\sum_{l=0}^{L-1} p_l = 1$ is satisfied.

The two-component mixture-Gaussian model considered in Sections II–V can be regarded as a special case of the general model (22) with parameters:

$$L = 2, \quad p_0 = 1 - p, \quad p_1 = p, \quad \sigma_0^2 = \sigma_w^2,$$
$$\sigma_1^2 = \sigma_w^2 + \sigma_g^2.$$

Another important special case of (22) is the Middleton Class A model [2], [3]. In this case, model parameters can be expressed as

$$L = \infty, \quad p_l = \frac{e^{-A} A^l}{l!},$$
$$\sigma_l^2 = \frac{l A^{-1} + \Gamma}{1 + \Gamma} \sigma_u^2, \quad l = 0, 1, \ldots, \infty$$

where σ_u^2 is the noise variance, A is the impulsiveness index, and Γ is the mean power ratio of the Gaussian noise component to the nonGaussian noise component [2], [3].

In case of the multicomponent mixture-Gaussian noise model, derivation of the K_0 and $E[|y_k|^2]$ is essentially the same as for the twocomponent model. The only difference is that now we must consider N mutually exclusive events $I_0, I_1, \ldots, I_{L-1}$ that represent the occurrence of noise samples with variance $\sigma_0^2, \sigma_1^2, \ldots, \sigma_{L-1}^2$, [22]. It is straightforward to show that in this case, the optimal scaling factor can be expressed as

$$K_0 = 1 - \sum_{l=0}^{L-1} \left(1 + \frac{T^2}{2(1+\sigma_l^2)}\right) p_l e^{-\frac{T^2}{2\left(1+\sigma_l^2\right)}} \tag{23}$$

and the variance of the noise samples at the output of blanking nonlinearity is given by

$$E[|y_k|^2] = 2 + \sum_{l=0}^{L-1} p_l \left(2\sigma_l^2 - \left[T^2 + 2\left(1+\sigma_l^2\right)\right] e^{-\frac{T^2}{2\left(1+\sigma_l^2\right)}}\right). \tag{24}$$

Similarly, the optimal blanking threshold (T_{opt}) is found as the solution of (18), which now can be expressed in compact form as

$$\frac{\sum_{l=0}^{L-1} \frac{p_l}{1+\sigma_l^2} e^{-\frac{T^2}{2\left(1+\sigma_l^2\right)}}}{2 + \sum_{l=0}^{L-1} p_l \left(2\sigma_l^2 - [T^2 + 2(1+\sigma_l^2)] e^{-\frac{T^2}{2\left(1+\sigma_l^2\right)}}\right)} - \frac{\sum_{l=0}^{L-1} \frac{p_l}{\left(1+\sigma_l^2\right)^2} e^{-\frac{T^2}{2\left(1+\sigma_l^2\right)}}}{1 - \sum_{l=0}^{L-1} p_l \left(1 + \frac{T^2}{2\left(1+\sigma_l^2\right)}\right) e^{-\frac{T^2}{2\left(1+\sigma_l^2\right)}}} = 0 \tag{25}$$

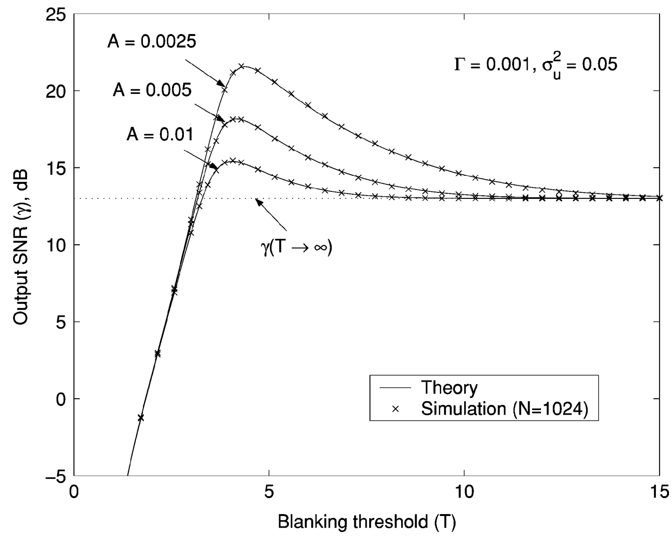

Fig. 8. SNR at the output of blanking nonlinearity versus threshold value for Class A (simulation results for 16-QAM system).

Fig. 8 shows the theoretical prediction obtained using (23) and (24) for the case of the Class A Middleton model and its comparison with simulation results. It can be seen that the theoretical prediction and simulation results are in very good agreement (Fig. 8).

VII. Conclusion

In this paper, closed-form expressions for performance characterization of the OFDM receiver with blanking nonlinearity in the presence of impulsive noise were derived. Simulation results show that the proposed analysis provides very good prediction of the output signal-to-noise ratio (SNR), and satisfactory approximation of the symbol-error rate (SER) if the number of OFDM subcarriers is sufficiently large. Based on this analysis, we propose a threshold optimization procedure. The analysis shows that there is a worst-case signal-to-impulsive noise ratio (SINR) that maximizes noise power in an OFDM receiver with blanking nonlinearity. The worst-case scenario corresponds to intermediate SINR values (-6 dB $\ldots -9$ dB, for given examples). It is shown that the poor performance of the OFDM receiver with blanking nonlinearity in the intermediate SINR region is mainly caused by imperfect detection of the signal samples affected by impulsive noise. An enhanced detection procedure may significantly improve overall performance of the OFDM receiver in an impulsive noise environment. This topic, along with improved SER estimation, is the subject for future research.

Appendix I

Derivation of $E[|s_k|^2 \,|\, \bar{C}, \bar{I}/I].\}$ To simplify notation, let us first introduce the following definitions:

$$A_s = |s_k|, \quad A_w = |w_k|, \quad A_y = |y_k|, \quad A_r = |r_k|.$$

Consider the case when the impulsive noise has not occurred. In this case, conditional expectation $E[A_s^2 \,|\, \bar{C}, \bar{I}]$ can be expressed as

$$E\left[A_s^2 \,|\, \bar{C}, \bar{I}\right] = \int_0^\infty A_s^2 f(A_s \,|\, \bar{C}, \bar{I})\, dA_s \tag{26}$$

where the conditional probability density function (PDF) $f(A_s \,|\, \bar{C}, \bar{I})$ can be found using Bayes' theorem as

$$\begin{aligned} f(A_s \,|\, \bar{C}, \bar{I}) &= f(A_s \,|\, A_r < T, \bar{I}) \\ &= \frac{f(A_s) P(A_r < T \,|\, A_s, \bar{I})}{P(A_r < T \,|\, \bar{I})}. \end{aligned} \tag{27}$$

Recalling that A_s has Rayleigh distribution with parameter $\sigma^2 = 1$, $f(A_s)$ can be expressed as

$$f(A_s) = A_s e^{-\frac{A_s^2}{2}}. \tag{28}$$

If the impulsive noise event has not occurred $(\bar{I})$, A_r has Rayleigh distribution with parameter $\sigma^2 = 1 + \sigma_w^2$. As a consequence, $P(A_r < T \,|\, \bar{I})$ can be expressed as

$$P(A_r < T \,|\, \bar{I}) = 1 - e^{-\frac{T^2}{2(1+\sigma_w^2)}}. \tag{29}$$

It is easy to show that the conditional PDF $f(A_r \,|\, A_s, \bar{I})$ is Rice-distributed with parameters $\alpha = A_s$ and $\sigma^2 = \sigma_w^2$, and the corresponding cumulative distribution function (CDF) can be expressed in terms of a Marcum Q-function [23, p. 46], i.e.,

$$P(A_r < T \,|\, A_s, \bar{I}) = 1 - Q_1\left(\frac{A_s}{\sigma_w}, \frac{T}{\sigma_w}\right) \tag{30}$$

where $Q_1(a, b)$ is the Marcum Q-function of the first order defined as

$$Q_1(a, b) = \int_b^\infty x e^{-\frac{x^2+a^2}{2}} I_0(ax)\, dx$$

and $I_0(x)$ is the modified Bessel function of the first kind.

Combining (27)–(36) yields

$$f(A_s \,|\, \bar{C}, \bar{I}) = \frac{A_s e^{-\frac{A_s^2}{2}}}{1 - e^{-\frac{T^2}{2(1+\sigma_w^2)}}} \left[1 - Q_1\left(\frac{A_s}{\sigma_w}, \frac{T}{\sigma_w}\right)\right]. \tag{31}$$

Substituting (31) into (26) gives

$$\begin{aligned} E\left[A_s^2 \,|\, \bar{C}, \bar{I}\right] &= \left(1 - e^{-\frac{T^2}{2(1+\sigma_w^2)}}\right)^{-1} \int_0^\infty A_s^3 e^{-\frac{A_s^2}{2}}\, dA_s \\ &- \left(1 - e^{-\frac{T^2}{2(1+\sigma_w^2)}}\right)^{-1} \int_0^\infty A_s^3 e^{-\frac{A_n^2}{2}} Q_1\left(\frac{A_s}{\sigma_w}, \frac{T}{\sigma_w}\right) dA_s. \end{aligned} \tag{32}$$

A straightforward calculation of the first integral on the right-hand side of (32) gives 2. The second integral can be expressed analytically using the results presented by Nuttall [28, (9)]. After simplification, $E[|s_k|^2 \,|\, \bar{C}, \bar{I}]$ can be expressed as

$$E[|s_k|^2 \,|\, \bar{C}, \bar{I}] = 2\left[1 - \frac{T^2}{2(1+\sigma_w^2)^2 \left\{e^{\frac{T^2}{2(1+\sigma_w^2)}} - 1\right\}}\right]. \tag{33}$$

It should be noted that the derivation of $E[|s_k|^2 \,|\, \bar{C}, I]$ is essentially the same as the derivation of $E[|s_k|^2 \,|\, \bar{C}, \bar{I}]$; the only difference is that in this case, additive noise power is $\sigma_w^2 + \sigma_g^2$. Therefore, $E[|s_k|^2 \,|\, \bar{C}, I]$ can be obtained using (33) by substituting $\sigma_w^2 \to \sigma_w^2 + \sigma_g^2$.

Derivation of $E[w_k s_k^* | \bar{C}, \bar{I}]$ *and* $E[(w_k + g_k) s_k^* \,|\, \bar{C}, I]$. To derive $E[w_k s_k^* \,|\, \bar{C}, \bar{I}]$, let us first note that $w_k s_k^*$ can be expressed as

$$w_k s_k^* = A_s A_w \cos\varphi - jA_s A_w \sin\varphi \tag{34}$$

where φ is the angle between vectors w_k and s_k; i.e., $\varphi = \arg(s_k) - \arg(w_k)$. Therefore

$$\begin{aligned} &E[w_k s_k^* | \bar{C}, \bar{I}] \\ &= E[A_s A_w \cos\varphi \,|\, \bar{C}, \bar{I}] - jE[A_s A_w \sin\varphi \,|\, \bar{C}, \bar{I}]. \end{aligned} \tag{35}$$

Note that the imaginary part of expectation $E[w_k s_k^* \,|\, \bar{C}, \bar{I}]$ is equal to zero, due to odd symmetry of the sinus function.

The direct derivation of $E[A_s A_w \cos\varphi \,|\, \bar{C}, \bar{I}]$ is a rather difficult task; instead, we can calculate it indirectly using the following geometrical equality:

$$A_y^2 = A_s^2 + A_w^2 + 2A_s A_w \cos\varphi. \tag{36}$$

Equation (36) immediately results in

$$\begin{aligned} &E[A_s A_w \cos\varphi \,|\, \bar{C}, \bar{I}] = \\ &\frac{1}{2} E\left[A_y^2 \,|\, \bar{C}, \bar{I}\right] - \frac{1}{2} E\left[A_s^2 \,|\, \bar{C}, \bar{I}\right] - \frac{1}{2} E\left[A_w^2 \,|\, \bar{C}, \bar{I}\right]. \end{aligned} \tag{37}$$

Note that we have already found $E[A_s^2 \,|\, \bar{C}, \bar{I}]$ (see (33)), and the derivation of $E[A_y^2 \,|\, \bar{C}, \bar{I}]$ is given in Appendix II. The remaining conditional expectation $E[A_w^2 \,|\, \bar{C}, \bar{I}]$ can be expressed as

$$E\left[A_w^2 \,\mid\, \bar{C}, \bar{I}\right] = \int_0^\infty A_w^2 f(A_w \,|\, \bar{C}, \bar{I})\, dA_w \tag{38}$$

where the conditional PDF $f(A_w \,|\, \bar{C}, \bar{I})$ is found using Bayes' theorem as

$$\begin{aligned} f(A_w \,|\, \bar{C}, \bar{I}) &= f(A_w \,|\, A_r < T, \bar{I}) \\ &= \frac{f(A_w) P(A_r < T \,|\, A_w, \bar{I})}{P(A_r < T \,|\, \bar{I})}. \end{aligned} \tag{39}$$

Recalling that A_w has Rayleigh distribution with parameter $\sigma^2 = \sigma_w^2$, $f(A_w)$ can be expressed as

$$f(A_w) = \frac{A_w}{\sigma_w^2} e^{-\frac{A_w^2}{2\sigma_w^2}}. \tag{40}$$

It is easy to show that the conditional PDF $f(A_r \mid A_w, \bar{I})$ is Rice-distributed with parameters $\alpha = A_w$ and $\sigma^2 = 1$, and the corresponding CDF is given by

$$P(A_r < T \mid A_w, \bar{I}) = 1 - Q_1(A_w, T). \tag{41}$$

Combining (40), (41), and (29) with (39) yields

$$f(A_w \mid \bar{C}, \bar{I}) = \frac{\frac{A_w}{\sigma_w^2} e^{-\frac{A_w^2}{2\sigma_w^2}}}{1 - e^{-\frac{T^2}{2(1+\sigma_w^2)}}} [1 - Q_1(A_w, T)]. \tag{42}$$

Substituting (42) into (38) gives

$$\begin{aligned} E[A_w \mid \bar{C}, \bar{I}] &= \frac{1}{\left(1 - e^{-\frac{T^2}{2(1+\sigma_w^2)}}\right) \sigma_w^2} \int_0^\infty A_w^3 e^{-\frac{A_w^2}{2\sigma_w^2}} dA_w \\ &\quad - \frac{1}{\left(1 - e^{-\frac{T^2}{2(1+\sigma_w^2)}}\right) \sigma_w^2} \\ &\quad \times \int_0^\infty A_w^3 e^{-\frac{A_w^2}{2\sigma_w^2}} Q_1(A_w, T) dA_w. \end{aligned} \tag{43}$$

A straightforward calculation of the first integral on the right-hand side of (43) gives $2\sigma_w^2$. The second integral can be expressed analytically using the results presented by Nuttall ([28], (9)). After simplification, $E[A_w \mid \bar{C}, \bar{I}]$ can be expressed as

$$E\left[A_w^2 \mid \bar{C}, \bar{I}\right] = 2\sigma_w^2 \left[1 - \frac{\sigma_w^2 T^2}{2\left(1 + \sigma_w^2\right)^2 \left\{e^{\frac{T^2}{2(1+\sigma_w^2)}} - 1\right\}}\right]. \tag{44}$$

Substituting (33), (44), and the result obtained in Appendix II into (37) gives

$$E[w_k s_k^* \mid \bar{C}, \bar{I}] = -\frac{T^2 \sigma_w^2}{\left(1 + \sigma_w^2\right)^2 \left\{e^{\frac{T^2}{2(1+\sigma_w^2)}} - 1\right\}}. \tag{45}$$

It is worth noting that the derivation of $E[(w_k + g_k)s_k^* \mid \bar{C}, I]$ is essentially the same as the derivation of $E[w_k s_k^* \mid \bar{C}, \bar{I}]$; the only difference is that, in this case, additive noise power is $\sigma_w^2 + \sigma_g^2$. Therefore, $E[(w_k + g_k)s_k^* \mid \bar{C}, I]$ can be obtained using (45) by substituting $\sigma_w^2 \to \sigma_w^2 + \sigma_g^2$.

APPENDIX II

Derivation of $E[|y_k|^2 \mid \bar{C}, \bar{I}/I]$. To derive $E[|y_k|^2 \mid \bar{C}, \bar{I}]$, we shall first express the conditional PDF $f(A_y \mid \bar{C}, \bar{I})$ as

$$f(A_y \mid \bar{C}, \bar{I}) = \begin{cases} \alpha \frac{A_y}{1+\sigma_w^2} e^{-\frac{A_y^2}{2(1+\sigma_w^2)}}, & 0 \le A_y \le T \\ 0, & \text{otherwise} \end{cases} \tag{46}$$

where α is the normalization constant found as

$$\alpha = \left(\int_0^T \frac{A_y}{1 + \sigma_w^2} e^{-\frac{A_y^2}{2(1+\sigma_w^2)}} dA_y\right)^{-1} = \left(1 - e^{-\frac{T^2}{2(1+\sigma_w^2)}}\right)^{-1}. \tag{47}$$

Last, $E[|y_k|^2 \mid \bar{C}, \bar{I}]$ can be expressed in closed form as

$$\begin{aligned} E[|y_k|^2 \mid \bar{C}, \bar{I}] &= \int_0^T A_y^2 f(A_y \mid \bar{C}, \bar{I}) \, dA_y \\ &= \alpha \int_0^T \frac{A_y^3}{1 + \sigma_w^2} e^{-\frac{A_y^2}{2(1+\sigma_w^2)}} \\ &= 2\left(1 + \sigma_w^2\right) - \frac{T^2}{e^{\frac{T^2}{2(1+\sigma_w^2)}} - 1}. \end{aligned} \tag{48}$$

Similarly, $E[|y_k|^2 \mid \bar{C}, I]$ can be obtained using (48) by substituting $\sigma_w^2 \to \sigma_w^2 + \sigma_g^2$.

ACKNOWLEDGMENT

The author would like to thank the anonymous reviewers for their valuable comments. He would also like to thank Mr. S. Salgar for careful proofreading of this manuscript.

REFERENCES

[1] J. A. C. Bingham, "Multicarrier modulation for data transmission: An idea whose time has come," *IEEE Commun. Mag.*, vol. 28, no. 5, pp. 5–14, May 1990.

[2] D. Middleton, "Statistical-physical models of electromagnetic interference," *IEEE Trans. Electromagn. Compat.*, vol. EMC-19, pp. 106–127, Aug. 1977.

[3] D. Middleton, "Canonical and quasi-canonical probability models of class A interference," *IEEE Trans. Electromagn. Compat.*, vol. EMC-25, pp. 76–106, May 1983.

[4] K. L. Blackard, T. S. Rappaport, and C. W. Bostian, "Measurement and models of radio frequency impulsive noise for indoor wireless communications," *IEEE J. Sel. Areas Commun.*, vol. 11, no. 9, pp. 991–1001, Sep. 1993.

[5] M. G. Sanchez *et al.*, "Impulsive noise measurements and characterization in a UHF digital TV channel," *IEEE Trans. Electromagn. Compat.*, vol. 41, no. 2, pp. 124–136, May 1999.

[6] W. R. Lauber and J. M. Bertrand, "Statistics of motor vehicle ignition noise at VHF/UHF," *IEEE Trans. Electromagn. Compat.*, vol. 41, no. 3, pp. 257–259, Aug. 1999.

[7] M. Ghosh, "Analysis of the effect of impulse noise on multicarrier and single carrier QAM systems," *IEEE Trans. Commun.*, vol. 44, no. 2, pp. 145–147, Feb. 1996.

[8] P. Lewis, "A tutorial on impulsive noise in COFDM systems," Digital Television Group (DTG) Monograph, Twickenham, London, UK, no. 5, 2001. [Online]. Available: http://www.dtg.org.uk

[9] O. P. Haffenden *et al.*, "Detection and removal of clipping in multicarrier receivers," Eur. Patent Application EP1043874, Bulletin 2000/41, Oct. 2000.

[10] N. P. Cowley, A. Payne, and M. Dawkins, "COFDM tuner with impulse noise reduction," Eur. Patent Application EP1180851, Bulletin 2002/08, Feb. 2002.

[11] S. S. Rappaport and L. Kurz, "An optimal nonlinear detector for digital data transmission through non-Gaussian channels," *IEEE Trans. Commun. Technol.*, vol. COM-14, pp. 266–274, Jun. 1966.

[12] O. Antonov, "Optimal detection of signals in non-Gaussian noise," *Radio Eng. Electron. Phys. (USSR)*, vol. 12, pp. 541–548, 1967.

[13] K. S. Vastola, "Threshold detection in narrow-band non-Gaussian noise," *IEEE Trans. Commun.*, vol. COM-32, no. 2, pp. 134–139, Feb. 1984.

[14] R. Ingram, "Performance of the locally optimum threshold receiver and several suboptimal nonlinear receivers for ELF noise," *IEEE J. Ocean. Eng.*, vol. OE-9, no. 3, pp. 202–208, Jul. 1984.

[15] A. D. Spaulding, "Locally optimum and suboptimum detector performance in a non-Gaussian interference environment," *IEEE Trans. Commun.*, vol. COM-33, pp. 509–517, Jun. 1985.

[16] H. A. Suraweera, C. Chai, J. Shentu, and J. Armstrong, "Analysis of impulse noise mitigation techniques for digital television systems," in *Proc. 8th Int. OFDM Workshop*, Hamburg, Germany, Sep. 2003, pp. 172–176.

[17] S. Wei, D. L. Goeckel, and P. E. Kelly, "A modern extreme value theory approach to calculating the distribution of the peak-to-average power ratio in OFDM systems," in *Proc. IEEE Int. Conf. Communications*, vol. 3, Apr./May 2002, pp. 1686–1690.
[18] P. Banelli and S. Cacopardi, "Theoretical analysis and performance of OFDM signals in nonlinear AWGN channels," *IEEE Trans. Commun.*, vol. 48, no. 3, pp. 430–441, Mar. 2000.
[19] J. Haring and A. J. Han Vinck, "Iterative decoding of codes over complex numbers for impulsive noise channels," *IEEE Trans. Inf. Theory*, vol. 49, no. 5, pp. 1251–1260, May 2003.
[20] S. V. Zhidkov, "Impulsive noise suppression in OFDM-based communication systems," *IEEE Trans. Consum. Electron.*, vol. 49, no. 4, pp. 944–948, Nov. 2003.
[21] A. Conti, D. Dardari, and V. Tralli, "An analytical framework for CDMA systems with a nonlinear amplifier and AWGN," *IEEE Trans. Commun.*, vol. 50, no. 7, pp. 1110–1120, Jul. 2002.
[22] S. A. Kassam, *Signal Detection in Non-Gaussian Noise*. Berlin, Germany: Springer-Verlag, 1988.
[23] J. Proakis, *Digital Communications*, 4th ed. New York: McGraw-Hill, 2001.
[24] D. Gianfelici, L. Franchina, and S. A. Kosmopoulos, "Symbol-to-symbol performance evaluation of densely populated asynchronous DS-CDMA in Gaussian and impulsive noise environments: A Fourier-Bessel series approach," *IEEE Trans. Commun.*, vol. 46, no. 7, pp. 866–869, Jul. 1998.
[25] H. Dai and H. V. Poor, "Crosstalk mitigation in DMT VDSL with impulse noise," *IEEE Trans. Circuits Syst.—I, Fundam. Theory Appl.*, vol. 48, no. 10, pp. 1205–1213, Oct. 2001.
[26] S. A. Kosmopoulos, P. T. Mathiopoulos, and M. D. Gouta, "Fourier-bessel error performance analysis and evaluation of M-ary QAM schemes in an impulsive noise environment," *IEEE Trans. Commun.*, vol. 39, no. 3, pp. 398–404, Mar. 1991.
[27] J. Tellado, L. M. C. Hoo, and J. M. Cioffi, "Maximum-likelihood detection of nonlinearly distorted multicarrier symbols by iterative decoding," *IEEE Trans. Commun.*, vol. 51, no. 2, pp. 218–228, Feb. 2003.
[28] A. H. Nuttall, "Some integrals involving the Q_M function," *IEEE Trans. Inf. Theory*, vol. IT-14, no. 1, pp. 95–96, Jan. 1975.

Sergey V. Zhidkov received the engineering and the Ph.D. degrees from Izhevsk State Technical University (ISTU), Izhevsk, Russia, in 1997 and 2000, respectively.

In 1997, he joined the Radio Engineering Department of ISTU as an Assistant Researcher, and from 2001 to 2002, he was an Assistant Professor at the same University. Since January of 2003, he joined Samsung Electronics Co, Ltd., Giheung, Korea, where he is presently a Senior Research Engineer with the System-On-Chip Reseach center. His current research interests include digital signal processing for wireless communications, multimedia broadcasting systems, OFDM, interference compensation techniques, and iterative equalization/decoding.

Dr. Zhidkov is a recipient of the ISTU Conscientious Teaching Award (ISTU, 2001), Samsung Young Scientist Award (Samsung Company and Siberian Branch of Russian Academy of Science, 2002), and Future Creator/Innovator Award (Samsung Electronics, 2005).